

1 **Direct Observation of Electrically Conductive Pili Emanating from**
2 ***Geobacter sulfurreducens***

3 Xinying Liu^{a,b}, David J. F. Walker^c, Stephen S. Nonnenmann^{d,e}, Dezhi Sun^b, Derek R. Lovley^{a,d}

4 ^a Department of Microbiology, University of Massachusetts—Amherst, Amherst, Massachusetts, USA

5 ^b College of Environmental Science and Engineering, Beijing Forestry University, Beijing, 100083, China

6 ^c Institute for Cellular and Molecular Biology, University of Texas at Austin, Austin, Texas 78712, USA

7 ^d Institute for Applied Life Sciences, university of Massachusetts—Amherst, Amherst, Massachusetts, USA

8 ^e Department of Mechanical and Industrial Engineering, University of Massachusetts—Amherst, Amherst,

9 Massachusetts, USA

10

11 **Abstract**

12 *Geobacter sulfurreducens* is a model microbe for elucidating the mechanisms for extracellular
13 electron transfer in several biogeochemical cycles, bioelectrochemical applications, and
14 microbial metal corrosion. Multiple lines of evidence previously suggested that electrically
15 conductive pili (e-pili) are an essential conduit for long-range extracellular electron transport in
16 *G. sulfurreducens*. However, it has recently been reported that *G. sulfurreducens* does not
17 express e-pili and that filaments comprised of multi-heme *c*-type cytochromes are responsible for
18 long-range electron transport. This possibility was directly investigated by examining cells,
19 rather than filament preparations, with atomic force microscopy. Approximately 90 % of the
20 filaments emanating from wild-type cells had a diameter (3 nm) and conductance consistent with
21 previous reports of e-pili harvested from *G. sulfurreducens* or heterologously expressed in *E. coli*
22 from the *G. sulfurreducens* pilin gene. The remaining 10% of filaments had a morphology
23 consistent with filaments comprised of the *c*-type cytochrome OmcS. A strain expressing a
24 modified pilin gene designed to yield poorly conductive pili expressed 90 % filaments with a 3
25 nm diameter, but greatly reduced conductance, further indicating that the 3 nm diameter
26 conductive filaments in the wild-type strain were e-pili. A strain in which genes for five of the
27 most abundant outer-surface *c*-type cytochromes, including OmcS, was deleted yielded only 3
28 nm diameter filaments with the same conductance as in the wild-type. These results demonstrate
29 that e-pili are the most abundant conductive filaments expressed by *G. sulfurreducens*, consistent
30 with previous functional studies demonstrating the need for e-pili for long-range extracellular
31 electron transfer.

32

33

34 **Importance**

35 Electroactive microbes have significant environmental impacts as well as applications in
36 bioenergy and bioremediation. The composition, function, and even existence of electrically
37 conductive pili (e-pili) has been one of the most contentious areas of investigation in
38 electromicrobiology, in part because e-pili offer a mechanism for long-range electron transport
39 that does not involve the metal co-factors common in much of biological electron transport. This
40 study demonstrates that e-pili are abundant filaments emanating from *Geobacter sulfurreducens*,
41 which serves as a model for long-range extracellular electron transfer in direct interspecies
42 electron transfer, dissimilatory metal reduction, microbe-electrode exchange, and corrosion
43 caused by direct electron uptake from Fe(0). The methods described in this study provide a
44 simple strategy for evaluating the distribution of conductive filaments throughout the microbial
45 world with an approach that avoids artifactual production and/or enrichment of filaments that
46 may not be physiologically relevant.

47

48

49 Electroactive microorganisms are important in multiple biogeochemical cycles, the human
50 gut, several bioenergy strategies, and metal corrosion (1, 2). One of the most contentious issues
51 in electromicrobiology has been the role of electrically conductive protein nanowires in
52 facilitating long-range electron transport. Electrically conductive protein nanowires have been
53 studied most extensively in *Geobacter sulfurreducens*, which has served as the model microbe
54 for elucidating the mechanisms of long-range electron transport in *Geobacter* species (3).
55 *Geobacter* are of interest because they are often the most abundant electroactive microbes in
56 soils and sediments in which organic matter oxidation is coupled to Fe(III) oxide reduction; in
57 natural methanogenic environments and anaerobic digesters where they serve as electron-
58 donating partners for direct interspecies electron transfer (DIET) with methanogens; and in
59 electrode biofilms harvesting electricity from waste organic matter (3-5). Furthermore,
60 *Geobacter* are the most effective microbes available in culture for extracellular electron transport
61 functions such as Fe(III) oxide reduction (3), producing electric current (5), DIET (6), and
62 corrosion via direct extraction of electrons from metallic iron (7, 8). An additional area of
63 interest is the potential for constructing electronic devices with novel functions with *G.*
64 *sulfurreducens* protein nanowires (9).

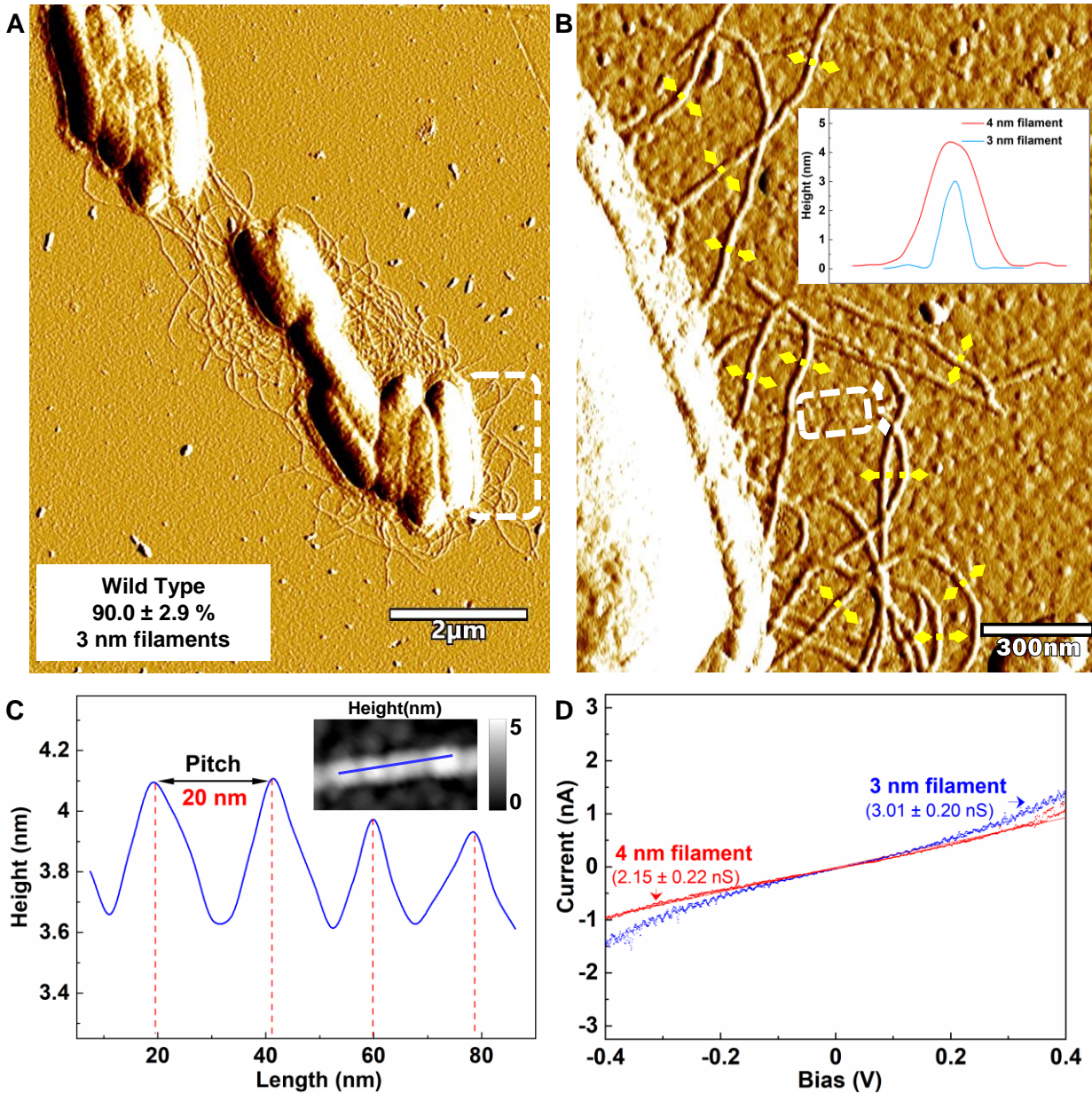
65 Debate has arisen over the composition of *G. sulfurreducens* protein nanowires and their
66 role in long-range electron transfer. Multiple lines of evidence have suggested that electrically
67 conductive pili (e-pili) are the most abundant *G. sulfurreducens* protein nanowires and that e-pili
68 are essential for long-range electron transport (10, 11). However, two recent publications have
69 suggested that *G. sulfurreducens* does not express e-pili and that protein nanowires comprised of
70 the multi-heme *c*-type cytochromes OmcS and OmcZ are the functional conduits for long-range
71 extracellular electron transfer (12, 13). The primary argument against the production of e-pili is

72 the fact filaments comprised of *c*-type cytochromes are the most abundant filaments observed in
73 filament preparations observed with cryo-electron microscopy (12, 13). However, generating
74 these filament preparations involves shearing filaments from the cell, purifying the filaments
75 under high pH, selective precipitation with ammonium sulfate, and affixing filaments to grids.
76 Each of these steps has the potential to selectively enrich specific filaments or for artifactual
77 formation of cytochrome filaments (11). For example, in studies of *G. sulfurreducens* filament
78 preparations prepared by the same person in the same laboratory, under identical conditions,
79 cryo-electron microscopy suggest that a majority of the filaments were comprised of OmcS (14),
80 whereas filaments with a diameter consistent with e-pili, not OmcS, were observed with atomic
81 force microscopy (AFM) (15).

82 **Direct AFM of Cells.**

83 In order to avoid potential artifacts/enrichments associated with filament purification, the
84 filaments associated with *G. sulfurreducens* cells were directly examined with AFM. To simplify
85 the analysis, cells were grown with fumarate as the electron acceptor, a growth condition in
86 which the pilin monomer PilA and OmcS are expressed, but expression of the gene for the multi-
87 heme cytochrome OmcZ is repressed (16-18). AFM of culture aliquots directly deposited on a
88 conductive surface revealed cells with abundant filaments (Fig. 1A and Supplemental Fig. S1A).
89 There were two types of filaments emanating from the cells. One filament type appeared to be
90 comprised of OmcS, as evidenced from its 4 nm diameter (Fig. 1B and Supplemental Fig. S1B)
91 and its characteristic axial periodicity with a 20 nm pitch (12, 14) (Fig. 1C). The OmcS
92 filaments consistently accounted for only ca. 10 % of the filaments observed (Fig.1A and
93 Supplemental Figs. S2-4).

94 Approximately 90% of the filaments were 3 nm in diameter (Fig. 1A and Supplemental
95 Figs. S2-4), the same diameter as the filaments observed when the *G. sulfurreducens* PilA gene
96 is expressed in *Pseudomonas aeruginosa* (19) or *Escherichia coli* (20) and the same diameter of
97 individual conductive filaments previously harvested from *G. sulfurreducens* (16, 21). These
98 results suggest that the 3 nm diameter filaments are e-pili. As expected from the growth
99 conditions employed, no filaments with a morphology consistent with the 2.5 nm diameter and
100 axial pitch of OmcZ filaments (13) were observed. Both the OmcS and e-pili filaments exhibited
101 an ohmic-like response (Fig. 1D). The conductance of the e-pili was slightly higher than that of
102 the OmcS filaments (Fig. 1D).



103

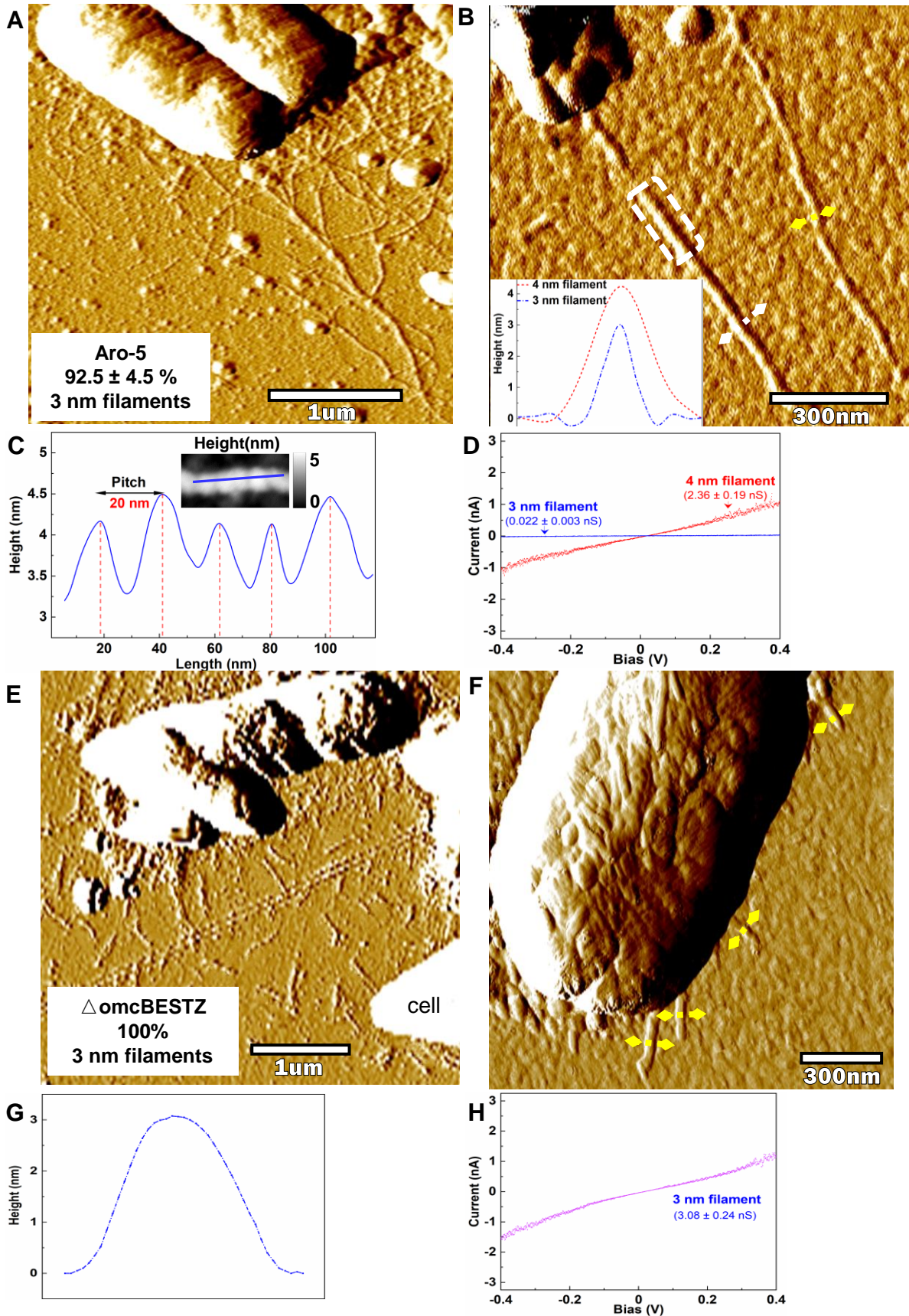
104 **Fig. 1. Characterization of filaments emanating from *G. sulfurreducens* with the wild-type**
105 **pilin gene. (A) AFM amplitude image. The proportion of 3 nm diameter filaments was**
106 **calculated from the total number of 3 nm and 4 nm diameter filaments counted in 9 regions**
107 **from 3 separate samples (Supplemental Figs. 2-4) and were determined from height images**
108 **similar to those shown in Supplemental Fig. 1. (B) Higher magnification of the region**
109 **highlighted in the dashed frame in panel A. Inset shows typical height profiles across the 3**
110 **nm (yellow lines) and 4 nm (white line) diameter filaments, as determined from the**
111 **corresponding height images (Supplemental Fig. S1B). Due to fluctuation of diameter along**
112 **the axis of the filaments, diameters were measured at the points of greatest diameter for**
113 **consistency. (C) Longitudinal height profile (along solid blue line in inset) for region on the**
114 **4 nm filament noted by the white dashed frame in panel B. (D) Comparison of point-mode**
115 **current response (I-V) spectroscopy for 4 nm (red) and 3 nm (blue) diameter filaments.**

116 **The responses shown are representative of three different measurements on each of three**
117 **individual filaments (Supplemental Figs. S5 and S6). Conductance (mean + standard**
118 **deviation, n=9) was calculated from a linear fit model between -0.2 V and 0.2 V**
119 **(Supplemental Figs. S5 and S6).**

120
121 *G. sulfurreducens* strain Aro-5 was previously constructed to replace the PilA pilin gene
122 with *aro-5*, a synthetic pilin gene designed to yield poorly conductive pili (18). The conductivity
123 of filaments harvested from the cells is much lower than the conductivity of filaments harvested
124 from wild-type controls (18, 21-23). Direct examination of filaments emanating from strain Aro-
125 5 revealed two types of filaments, morphologically similar to those observed in the wild-type
126 control (Figs. 2A, B and Supplemental Fig. S1C, D). Filaments with a diameter and longitudinal
127 pitch (Fig. 2C) consistent with OmcS filaments comprised ca. 10 % of the filaments (Fig. 2A,
128 Supplemental Figs. S7 and S8), similar to the OmcS filament abundance in the wild-type control
129 and consistent with the observation that strain Aro-5 produces abundant OmcS (18). The
130 conductance of these 4 nm diameter filaments was the same as the conductance observed for the
131 OmcS filaments of the wild-type control (Fig. 2D and Supplemental Fig. S9). As with the wild-
132 type strain, the 3 nm diameter filaments accounted for ca. 90% of the filaments observed, but
133 their conductance was more than 100-fold lower (Fig. 2D and Supplemental Fig. S10). This
134 decreased conductance is in agreement with previous observations of attenuated conductivity in
135 filaments harvested from strain Aro-5, including measurements on individual 3 nm diameter
136 filaments (18, 21-23). The dramatic change in the conductance of the 3 nm filaments emanating
137 from cells associated with the expression of *aro-5* pilin gene provides further evidence that the 3
138 nm filaments in the wild-type strain were e-pili.

139 In order to further investigate the possibility of cytochrome-based filaments, we next
140 examined the previously described strain Δ omcBESTZ (24) in which the genes for the most
141 abundant *G. sulfurreducens* outer surface multi-heme c-type cytochromes, OmcB, OmcE, OmcS,

142 OmcT, and OmcZ were deleted. As expected, filaments with morphologies consistent with
143 OmcS-based filaments were not apparent in this strain. All of the filaments emanating from
144 strain Δ omcBESTZ and lying near the cells were short, but had a diameter of 3 nm (Fig. 2E, F
145 and Supplemental Fig. S1E, F). Their conductance was the same as for the 3 nm filaments of the
146 wild-type strain (Fig. 2H, Supplemental Fig. S11).



148 **Fig. 2. Characterization of filaments emanating from *G. sulfurreducens* strain Aro-5 and**
149 **strain Δ omcBESTZ. (A) AFM amplitude image of filaments associated with strain Aro-5.**
150 **The proportion of 3 nm diameter filaments was calculated from the total number of 3 nm**
151 **and 4 nm diameter filaments counted in 6 regions from 3 separate samples (Supplemental**
152 **Figs. S7 and S8) and were determined from height images similar to those shown in**
153 **Supplemental Fig. 1. (B) AFM amplitude image at higher magnification illustrating the two**
154 **filament types. Inset shows typical height profiles across the 3 nm (yellow lines) and 4 nm**
155 **(white line) diameter filaments, as determined from the corresponding height images**
156 **(Supplementary Fig. 1D). (C) Longitudinal height profile (along solid blue line in inset) for**
157 **the portion of the 4 nm diameter filament within the white frame in panel B. (D)**
158 **Comparison of point-mode current response (I-V) spectroscopy for 4 nm (red) and 3 nm**
159 **(blue) filaments. The responses shown are representative of three different measurements**
160 **on three individual wires (Supplemental Figs. S9 and S10). Conductance (mean + standard**
161 **deviation, n=9) was calculated from a linear fit model between -0.2 V and 0.2 V**
162 **(Supplemental Figs. S9 and S10). (E) AFM amplitude image of filaments associated with**
163 **strain Δ omcBESTZ. (F) AFM amplitude image at higher magnification showing 3 nm**
164 **diameter filaments emanating from cell of strain Δ omcBESTZ. (G) Typical height profile**
165 **across the filaments designated by yellow lines in panel F, as determined from the**
166 **corresponding height images (Supplementary Fig. 1F). (H) Point-mode current response (I-**
167 **V) spectroscopy representative of three different measurements on three individual wires**
168 **(Supplemental Fig. S11) on 3 nm filaments emanating from strain Δ omcBESTZ.**
169 **Conductance (mean + standard deviation, n=9) was calculated from a linear fit model**
170 **between -0.2 V and 0.2 V (Supplemental Fig. S11).**

171 172 **Implications.**

173 The results of direct observation of filaments emanating from cells of *G. sulfurreducens*
174 demonstrates that *G. sulfurreducens* copiously expresses filaments with properties expected for
175 e-pili. The e-pili were ca. 10-fold more abundant than putative OmcS filaments. These
176 observations are in accordance with a number of previous observations. For example, when a
177 pilin monomer modified with a peptide tag was expressed in *G. sulfurreducens* all of the
178 filaments observed emanating from the cells were also decorated with the peptide tag (25).
179 Several studies reported recovery of electrically conductive 3 nm diameter filaments when
180 filaments were sheared off the outer surface of *G. sulfurreducens* (16, 21, 25) or when the *G.*
181 *sulfurreducens* pilin monomer was expressed in *P. aeruginosa* (19) or *E. coli* (20). Furthermore,
182 as shown here, expressing *aro-5* instead of PilA resulted in 3 nm filaments emanating from the
183 cells with a similar morphology, but greatly attenuated conductance. Heterologously expressing

184 a pilin gene encoding increased aromatic amino acid content yielded 3 nm diameter filaments
185 with 5000-fold higher conductivity than the wild-type control (26). These results are consistent
186 with the expression of e-pili and inconsistent with cytochrome-based filaments, as was the
187 finding reported here that the 3 nm filaments were still produced in a strain in which the genes
188 for all the most abundant outer-surface cytochromes were deleted. The abundance of e-pili in *G.*
189 *sulfurreducens* is also consistent with the finding that microbes that do not express outer-surface
190 c-type cytochromes can construct conductive filaments from monomers homologous to the *G.*
191 *sulfurreducens* pilin monomer (22, 23, 27).

192 Notably, *G. sulfurreducens* strains that express pili of low conductance are consistently
193 deficient in long-range extracellular electron transfer (18, 22, 28), providing strong evidence for
194 the role of e-pili in extracellular electron transport. The same cannot be said of the cytochrome
195 filaments OmcS and OmcZ. *G. sulfurreducens* strain Aro-5 cannot produce highly conductive
196 biofilms or high current densities on anodes (18), whereas deleting *omcS* has no impact on these
197 phenotypes (17, 29). Deletion of *omcS* can inhibit Fe(III) oxide reduction, in some, but not all
198 variants of *G. sulfurreducens* (30, 31). When deletion of *omcS* does have an impact, the strain
199 can be rescued for Fe(III) oxide reduction with the addition of ultrafine-grained magnetite (32).
200 However, magnetite cannot substitute for e-pili, demonstrating an essential role for e-pili in
201 Fe(III) oxide reduction, but not for OmcS. OmcZ is not required for Fe(III) oxide reduction (17)
202 and is not highly expressed in cells reducing Fe(III) oxide (30). Although it was suggested that
203 OmcZ filaments might account for the high conductivity of anode biofilms (13), this hypothesis
204 is inconsistent with the poor current production by strain Aro-5 and the low conductivity of its
205 biofilms (18). Furthermore, OmcZ is localized near the anode-biofilm interface, OmcZ filaments
206 are not observed coursing through the bulk of the biofilm (33).

207 In conclusion, eliminating artifacts by directly examining filaments emanating from cells
208 has demonstrated that *G. sulfurreducens* expresses e-pili in abundance, consistent with multiple
209 lines of evidence from previous studies (10, 11) that have indicated that *G. sulfurreducens* e-pili
210 are an important component in long-range extracellular electron transport. The cells examined
211 produced few OmcS-based filaments. The physiological significance of cytochrome-based
212 filaments is yet to be determined.
213

214 **Methods**

215 **Culture source and growth conditions.**

216 The strain of *G. sulfurreducens* expressing wild-type PilA pilin gene as well as strain Aro-5,
217 which expresses a synthetic pilin gene designed to yield poorly conductive pili, and strain
218 Δ omcBESTZ, which features deletions in five major outer-surface *c*-type cytochromes, were
219 obtained from our laboratory culture collection and were previously described in detail (18, 24).
220 Cells were grown in medium with acetate (10 mM) as electron donor and fumarate (40 mM) as
221 electron acceptor as previously described (34). Cultures for AFM analysis were grown in the
222 acetate-fumarate medium at 25 °C, a condition known to promote expression of e-pili (16).

223 **Analysis with atomic force microscopy.**

224 An aliquot (50 μ l) of culture was drop cast onto a silicon wafer coated with a 35 nm layer of
225 platinum, prepared as previously described (35). After 12 min, excess liquid was removed with a
226 pipette and the substrate was washed twice with 50 μ l of deionized water. Excess water was
227 absorbed with filter paper and the preparation was allowed to air dry. Samples were equilibrated
228 at 40% humidity inside scanning chamber of a Cypher ES, atomic force microscope (Asylum
229 Research, Oxford Instrument) for at least 1 h at 25 °C. The filaments were first observed with
230 tapping mode (AC-air topography) under repulsive force with a Pt/Ir-coated tip (PtSi-FM,
231 NanoWorld AG) at a \sim 2.0 N/m spring force constant and \sim 70 kHz resonance frequency.

232 The conductance of individual filaments was determined in contact mode (force 30 nN)
233 with the Pt/Ir-coated tip functioning as the translatable top electrode. Quadruplicate amplitude of
234 \pm 0.4 V voltage at 0.99 Hz frequency was applied to get ca.8000 points per measurement. Three
235 independent points from three individual wire (biological replicates) were analyzed to determine

236 the conductance. Conductance was calculated from the linear slope between -0.2 to 0.2 V
237 followed with the equation: $\text{Conductance} = \text{Current}/\text{Voltage}$ as preciously described (23).

238

References

- 239 1. Shi L, Dong H, Reguera G, Beyenal H, Lu A, Liu J, Yu H-Q, Fredrickson JK. 2016.
240 Extracellular electron transfer mechanisms between microorganisms and minerals.
241 *Nature Reviews Microbiology* 14:651-662.
- 242 2. Lovley DR, Holmes DE. 2021. Electromicrobiology: The ecophysiology of
243 phylogenetically diverse electroactive microorganisms. *Nature Reviews Microbiology*
244 19:(in press).
- 245 3. Lovley DR, Ueki T, Zhang T, Malvankar NS, Shrestha PM, Flanagan K, Aklujkar M,
246 Butler JE, Giloteaux L, Rotaru A-E, Holmes DE, Franks AE, Orellana R, Risso C, Nevin
247 KP. 2011. *Geobacter*: the microbe electric's physiology, ecology, and practical
248 applications. *Adv Microb Physiol* 59:1-100.
- 249 4. Zhao Z, Li Y, Zhang Y, Lovley DR. 2020. Sparking anaerobic digestion: promoting
250 direct interspecies electron transfer to enhance methane production. *iScience* 23:101794.
- 251 5. Logan BE, Rossi R, Ragab A, Saikaly PE. 2019. Electroactive microorganisms in
252 bioelectrochemical systems. *Nature Reviews Microbiology* 17:307-319.
- 253 6. Lovley DR. 2017. Syntrophy goes electric: direct interspecies electron transfer. *Ann Rev*
254 *Microbiol* 71:643-664.
- 255 7. Tang H-Y, Yang C, Ueki T, Pittman CC, Xu D, Woodard TL, Holmes DE, Gu T, Wang
256 F, Lovley DR. 2021. Direct metal-microbe electron transfer is required for microbial
257 corrosion of stainless steel. *ISME J* 15:<https://doi.org/10.1038/s41396-021-00990-2>.
- 258 8. Tang H-Y, Holmes DE, Ueki T, Palacios PA, Lovley DR. 2019. Iron corrosion via direct
259 metal-microbe electron transfer. *mBio* 10:e00303-19.
- 260 9. Lovley DR, Yao J. 2021. Intrinsically conductive microbial nanowires for 'green'
261 electronics with novel functions. *Trends in Biotechnology*
262 <https://doi.org/10.1016/j.tibtech.2020.12.005>
- 263 10. Lovley DR, Holmes DE. 2020. Protein Nanowires: The Electrification of the Microbial
264 World and Maybe Our Own. *J Bacteriol* 202:e00331-20.
- 265 11. Lovley DR, Walker DJF. 2019. *Geobacter* protein nanowires. *Frontiers in Microbiology*
266 10:2078.
- 267 12. Wang F, Gu Y, O'Brien JP, Yi SM, Yalcin SE, Srikanth V, Shen C, Vu D, Ing NL,
268 Hochbaum AI, Egelman EH, Malvankar NS. 2019. Structure of microbial nanowires
269 reveals stacked hemes that transport electrons over micrometers. *Cell* 177:361–369.
- 270 13. Yalcin SE, O'Brien JP, Gu Y, Reiss K, Yi SM, Jain R, Srikanth V, Dahl DJ, Huynh W,
271 Vu D, Acharya A, Chaudhuri S, Varga T, Batista VS, Malvankar NS. 2020. Electric field
272 stimulates production of highly conductive microbial OmcZ nanowires. *Nature Chemical*
273 *Biology* 16:1136–1142.
- 274 14. Filman DJ, Marino SF, Ward JE, Yang L, Mester Z, Bullitt E, Lovley DR, Strauss M.
275 2019. Cryo-EM reveals the structural basis of long-range electron transport in a
276 cytochrome-based bacterial nanowire. *Communications Biology* 2:219.
- 277 15. Fu T, Liu X, Gao H, Ward JE, Liu X, Yin B, Wang Z, Zhuo Y, Walker DJF, Yang J,
278 Chen J, Lovley DR, Yao J. 2020. Bioinspired bio-voltage memristors. *Nature*
279 *Communications* 11:1861.
- 280 16. Reguera G, McCarthy KD, Mehta T, Nicoll JS, Tuominen MT, Lovley DR. 2005.
281 Extracellular electron transfer via microbial nanowires. *Nature* 435:1098-1101.

- 282 17. Nevin KP, Kim B-C, Glaven RH, Johnson JP, Woodard TL, Methé BA, DiDonato Jr RJ,
283 Covalla SF, Franks AE, Liu A, Lovley DR. 2009. Anode biofilm transcriptomics reveals
284 outer surface components essential for high current power production in *Geobacter*
285 *sulfurreducens* fuel cells. PLoS ONE 4:e5628.
- 286 18. Vargas M, Malvankar NS, Tremblay P-L, Leang C, Smith JA, Patel P, Snoeyenbos-West
287 O, Nevin KP, Lovley DR. 2013. Aromatic amino acids required for pili conductivity and
288 long-range extracellular electron transport in *Geobacter sulfurreducens* mBio 4:e00105-
289 13. .
- 290 19. Liu X, Wang S, Xu A, Zhang L, Liu H, Ma LZ. 2019. Biological synthesis of high-
291 conductive pili in aerobic bacterium *Pseudomonas aeruginosa*. Appl Microbiol
292 Biotechnol 103:1535-1544.
- 293 20. Ueki T, Walker DJF, Woodard TL, Nevin KP, Nonnenmann S, Lovley DR. 2020. An
294 *Escherichia coli* chassis for production of electrically conductive protein nanowires. ACS
295 Synthetic Biology 9:647-654.
- 296 21. Adhikari RY, Malvankar NS, Tuominen MT, Lovley DR. 2016. Conductivity of
297 individual *Geobacter* pili. RSC Advances 6:8354-8357.
- 298 22. Walker DJF, Adhikari RY, Holmes DE, Ward JE, Woodard TL, Nevin KP, Lovley DR.
299 2018. Electrically conductive pili from genes of phylogenetically diverse
300 microorganisms. ISME J 12:48-58.
- 301 23. Walker DJF, Martz E, Holmes DE, Zhou Z, Nonnenmann SS, Lovley DR. 2019. The
302 archaeum of *Methanospirillum hungatei* is electrically conductive. mBio 10:e00579-19.
- 303 24. Voordeckers JW, Izallalen M, Kim B-C, Lovley DR. 2010. Role of *Geobacter*
304 *sulfurreducens* outer surface c-type cytochromes in the reduction of soil humic acid and
305 the humics analog anthraquinone-2,6-disulfonate. Appl Environ Microbiol 76:2371-2375.
- 306 25. Ueki T, Walker DJF, Tremblay P-L, Nevin KP, Ward JE, Woodard TL, Nonnenmann SS,
307 Lovley DR. 2019. Decorating the outer surface of microbially produced protein
308 nanowires with peptides. ACS Synthetic Biology 8:1809-1817.
- 309 26. Tan Y, Adhikari RY, Malvankar NS, Ward JE, Woodard TL, Nevin KP, Lovley DR.
310 2017. Expressing the *Geobacter metallireducens* PilA in *Geobacter sulfurreducens* yields
311 pili with exceptional conductivity. mBio 8:e02203-16.
- 312 27. Walker DJF, Nevin KP, Nonnenmann SS, Holmes DE, Woodard TL, Ward JE, Rotaru A-
313 E, Mcinerney MJ, Lovley DR. 2020. Syntrophus conductive pili demonstrate that
314 common hydrogen-donating syntrophs can have a direct electron transfer option. ISME J
315 14:837-846.
- 316 28. Liu X, Tremblay P-L, Malvankar NS, Nevin KP, Lovley DR, Vargas M. 2014. A
317 *Geobacter sulfurreducens* strain expressing *Pseudomonas aeruginosa* type IV pili
318 localizes OmcS on pili but Is deficient in Fe(III) oxide reduction and current production.
319 Appl Environ Microbiol 80:1219-1224.
- 320 29. Malvankar NS, Tuominen MT, Lovley DR. 2012. Lack of involvement of c-type
321 cytochromes in long-range electron transport in microbial biofilms and nanowires.
322 Energy Environ Sci 5:8651 - 8659.
- 323 30. Mehta T, Coppi MV, Childers SE, Lovley DR. 2005. Outer membrane c-type
324 cytochromes required for Fe(III) and Mn(IV) oxide reduction in *Geobacter*
325 *sulfurreducens*. Appl Environ Microbiol 71:8634-8641.

- 326 31. Walker DJF, Li Y, Meier D, Pinches S, Holmes DE, Smith JA. 2020. Cytochrome OmcS
327 is not essential for long-range electron transport in *Geobacter sulfurreducens* strain
328 KN400. bioRxiv:doi: <https://doi.org/10.1101/2020.07.22.214791>.
- 329 32. Liu F, Rotaru A-E, Shrestha PM, Malvankar NS, Nevin KP, Lovley DR. 2015. Magnetite
330 compensates for the lack of a pilin-associated c-type cytochrome in extracellular electron
331 exchange. *Environ Microbiol* 17:648-655.
- 332 33. Inoue K, Leang C, Franks AE, Woodard TL, Nevin KP, Lovley DR. 2010. Specific
333 localization of the c-type cytochrome OmcZ at the anode surface in current-producing
334 biofilms of *Geobacter sulfurreducens*. *Environ Microbiol Rep* 3:211-217.
- 335 34. Coppi MV, Leang C, Sandler SJ, Lovley DR. 2001. Development of a genetic system for
336 *Geobacter sulfurreducens*. *Appl Environ Microbiol* 67:3180-3187.
- 337 35. Zhou Z, López-Domínguez P, Abdullah M, Barber DM, Meng X, Park J, Van Driessche
338 I, Schiffman JD, Crosby AJ, Kittilstved KR, Nonnenmann SS. 2021. Memristive
339 behavior of mixed oxide nanocrystal assemblies. *ACS Applied Materials & Interfaces*
340 13:21635-21644.
341